Environmental Science and Pollution Research (2023) 30:31294–31308
https://doi.org/10.1007/s11356-022-24403-9

RESEARCH ARTICLE

Adsorption of chlorophenols on activated pine sawdust-activated carbon from solution in batch mode

Yuwei Song[1] · Yuanyuan Wang[1] · Runping Han[1]

Received: 1 September 2022 / Accepted: 21 November 2022 / Published online: 29 November 2022

Abstract

In this work, a novel adsorbent, activated carbon (PSAC) developed by the activation of pine sawdust's pyrolytic carbon (PSPC), is applied to adsorb 2,4-dichlorophenol (2,4-DCP) and 4-chlorophenol (4-CP). The optimized preparation conditions of PSAC were presented. The results revealed that equilibrium adsorption capacity (q_e) of PSAC was notably enhanced up to threefold compared with PSPC. The adsorbents were characterized by a variety of techniques such as SEM, XRD, FT-IR, and elemental analysis. The key factors (such as adsorbent dosage, pH, salt concentration, temperature, and contact time) influencing the adsorption process were also studied. The adsorption quantities of PSAC for 2,4-DCP and 4-CP were 135.7 mg·g^{-1} and 77.3 mg·g^{-1}, respectively. The equilibrium adsorption of 4-DCP and 4-CP was suitable to be predicted by the Freundlich and Koble-Corrigan models, while kinetic process was better described by the pseudo-second-order kinetic model and Elovich equation. The process was spontaneous. After repeated regeneration of PSAC with ethanol, the adsorption capacity of PSAC was not significantly reduced, indicating that PSAC can be recycled by regeneration after adsorption of 4-CP. This work provides a viable method to use activated carbon as an effective adsorbent for pollutant removal.

Keywords Adsorption · Activated carbon · 2,4-dichlorophenol · 4-chlorophenol · Regeneration

Introduction

Along with the development of society, problems of water pollution are increasingly serious. Among various water contaminants, such as dyes, toxic heavy metals, and organic compounds, chlorophenols have attracted extensive attention due to their high toxicity, carcinogenicity, teratogenicity, mutagenicity, and difficulties of degradation (Fang et al. 2018; Quan et al. 2004; Sun et al. 2019). The chlorophenols chemicals 2,4-dichlorophenol (2,4-DCP) and 4-chlorophenol (4-CP) are frequently employed as solvents for refined mineral oil to create colors, medications, and pesticides, etc. (Nasser and Mingelgrin 2014; Sun et al. 2019). The wastewater discharged from these industries often contains a certain amount of chlorophenol compounds. Therefore, it is urgent to develop effective treatment methods for the removal of 2,4-DCP and 4-CP.

In order to remove chlorophenols from wastewater, in recent years, many methods have been developed to solve this problem, such as adsorption, photocatalysis, heterogeneous catalysis, and solvent extraction (Garba et al. 2019; Hu et al. 2021b; Ramos-Ramirez et al. 2020; Tobiszewski et al. 2019). Each water treatment method has its own advantages and disadvantages, and the most suitable method should be selected according to different actual situations. Adsorption is one of the most commonly used water treatment methods at present (Duan et al. 2020; Varsha et al. 2022; Wang et al. 2022a).

Commercial activated carbon is effective to remove refractory pollutants from wastewater, but it is not low-cost, and the regeneration of exhausted activated carbon is difficult with some loss of mass. So attentions have been focused on the development of low cost adsorbent. Ahmed et al. (Ahmed and Theydan 2013) used the pods of Albizia japonica as raw material and prepared activated carbon

Responsible Editor: Tito Roberto Cadaval Jr

✉ Runping Han
rphan67@zzu.edu.cn

Yuwei Song
1542682693@qq.com

Yuanyuan Wang
2305942027@qq.com

[1] College of Chemistry, Zhengzhou University, No 100 of Ke Xue Road, Zhengzhou 450001, People's Republic of China

by microwave activation, which had a good adsorption and removal effect on 4-CP. By the possible acid–base interactions between $–NH_2$ on adsorbents and –OH in chlorophenols, Ghaffari et al. (Ghaffari et al. 2014) used an amine-modified ordered nanoporous silicon material as a new type of adsorbent to remove 2-chlorophenol in water with good results. Wang et al. (Wang et al. 2022b) prepared cetylpyridinium chloride-modified pine sawdust (CPC-PS) to adsorb 2,4-DCP adsorption. Compared to the raw pine sawdust, the CPC-PS improved the maximum adsorption capacity for 2,4-DCP by approximately 122%, which indicates this material is an effective material for 2,4-DCP removal.

The use of fossil fuels, which occupy a large proportion of the social energy structure, will produce a large amount of greenhouse gases and other pollutants, causing serious environmental pollution. Therefore, in light of environmental issues and the current energy crisis, the broad use of green and renewable biomass energy is becoming increasingly crucial. Agricultural and forestry wastes, animal manure produced in animal husbandry, and lignocellulose contained in straw and trees are the main sources of biomass with the qualities of repeatability, low pollution, and wide distribution (Zhao et al. 2019). Sawdust or wood waste mostly comprises cellulose (45–50%), lignin (23–30%), hemicellulose (20–30%), and various extractives (acids, soluble sugar, resins, waxes, oil, etc.) (1.5–5%), which contain abundant functional groups, for instance, hydroxyls, phenols, and carboxyls. Hence, sawdust can be used as a promising adsorbent. Ozacar et al. applied pine sawdust with just a simple cleaning to the adsorption of metal complex dyes, and the results showed that pine sawdust has considerable potential for the removal of metal complex dyes from aqueous solution over a wide range of concentrations. The monolayer adsorption capacities are 280.3 and 398.8 mg dye per g of pine sawdust for metal complex blue and metal complex yellow, respectively (Ozacar and Sengil 2005). Yang et al. used hydrothermal pressure pretreatment for pyrolysis/activation of pine sawdust without using any commercial chemical reagents. Adsorption experiences with perfluorooctanoic acid (PFOA) and methylene blue (MB) showed that the adsorption capacity of the prepared activated carbon was significantly better than that of commercial activated carbon (CAC (Yang and Cannon 2021). Pyrolysis of biochar can improve its adsorption capacity. Mannaï investigated the ability of raw sawdust, and its derived biochars obtained after pyrolysis to remove Cu(II) from water. The adsorption capacity of the sawdust for Cu(II) was significantly improved after pyrolysis, which was 3.4 times higher than that before pyrolysis.(Mannai et al. 2022) Moreover, chemical modification methods can also improve the adsorption capacity of sawdust. Małgorzata Wi´sniewska et al. prepared micro-mesoporous activated biocarbons from waste plum stones, pine sawdust, and horsetail herb by chemical modification. Among them, the plum stones-based activated biocarbon with the largest surface area (2759 m^2/g) showed excellent adsorption performance for two heavy metal ions, lead(II) and copper(II), with an adsorption capacity of about 180 mg/g (Mallakpour et al. 2021). Both pine sawdust itself and its derivatives are expected to achieve good results in the adsorption of pollutants.

In this study, one new adsorbent, activated carbon (PSAC) obtained by the activation of activated pyrolytic carbon from pine sawdust (PSPC), is selected to adsorb 2,4-DCP and 4-CP from solution. The adsorbents were characterized by a variety of techniques such as SEM, XRD, FT-IR and elemental analysis, and their adsorptive abilities were investigated. And the key factors (such as adsorbent dosage, pH, salt concentration, temperature, and contact time) influencing the adsorption process were also studied. What's more, the kinetic and thermodynamic analyses were also performed. This work provides a viable method to use activated carbon as an effective adsorbent for pollutant removal.

Materials and methods

Materials

Pine sawdust pyrolysis carbon (PCPS): The raw material, the solid residue obtained during the biomass refining process, was taken from a laboratory of the College of Chemistry of Zhengzhou University. The raw material went through numerous rounds of deionized water washing before being dried at 353 K. Then it was sieved to pick out particles of 60–80 mesh. Next put it into 5% hydrochloric acid, and boiled for 1 h to get rid of the impurities. After rinsing it with deionized water until it was neutral, dried it to obtain spare pyrolysis carbon named as PSPC.

2,4-DCP and 4-CP were chemically pure. And other commonly used chemical reagents such as ammonium chloride (NH_4Cl), sodium chloride (NaCl), hydrochloric acid, sodium sulfate (Na_2SO_4), and sodium hydroxide (NaOH), were of analytical grade.

Preparation of adsorbent

A certain amount of PSPC was immersed in NH_4Cl solution and activated by heating in a muffle furnace to prepare PSAC. The optimization of preparation conditions mainly considered factors such as NH_4Cl concentration, activation temperature, and activation time.

The detailed process of the preparation of absorbents was recorded in the Supplementary information.

Characterization

The characterization of materials is performed using various techniques, such as Fourier transform infrared spectroscopy (FTIR), scanning electron microscopy (SEM), and X-ray powder diffraction (XRD). The methods were presented in the Supplementary information.

Adsorption experiments

Batch adsorption experiments were conducted in this study. For this purpose, 0.010 g of PSAC was added into a 50-mL conical flask with 10 mL of 2,4-DCP (100 $mg{\cdot}L^{-1}$) or 4-CP (50 $mg{\cdot}L^{-1}$) solution. The experimental flask was placed into a thermoshaker at 303 K and 120 rpm for some time.

The processes in detail were shown in the Supplementary information.

UV–vis spectroscopic measurements were carried out to determine the concentrations of 2,4-DCP and 4-CP left in supernatant solutions referring to the standard curve of 2,4-DCP and 4-CP at the maximum wavelength of 285 nm and 225 nm. The quantity of adsorbate adsorbed onto per unit weight of PSAC (q_e, $mg{\cdot}g^{-1}$) and the removal rate of adsorbate in water (p, %) were estimated using Eq. 1 and Eq. 2 in Table S1.

The adsorption experiments were carried out twice and the average results were recorded. The error was less than 5%.

Adsorption isotherms and kinetics

The adsorption isotherm refers to the relationship between the amount of adsorbate in the solid phase and the adsorbate concentration in the liquid phase when the adsorption reaches equilibrium at a certain temperature. Through the fitting of the isotherm model, the adsorption mechanism can be simply inferred (De Castro et al. 2018). And it has a certain guiding significance for the setting of adsorption conditions in practical water treatment. In this study, four isothermal adsorption models (Langmuir, Freundlich, Temkin, and Koble-Corrigan) were used, and their equations and descriptions were presented in Table S1 (Eqs. 3–6) (Chen et al. 2022).

In the solid–liquid two-phase adsorption, the adsorption capacity of the adsorbent will change with the increase of the contact time between the adsorbent and the adsorbate solution, which is reflected by adsorption kinetic curve (Mpatani et al. 2020a). From the adsorption kinetic curve, the rate change of the adsorption reaction and the time required to reach the adsorption equilibrium can be seen to some extent. The adsorption mechanism can be simply inferred by fitting the commonly used models. The models used in the study were pseudo-second-order kinetic model, Elovich equation, and intraparticle diffusion model and were presented in Table S1 (Eqs. 7–9).

Desorption and regeneration

The detailed desorption and regeneration process was recorded in the Supplementary information. The desorption rate d and the regeneration rate r were calculated from the formulas in Table S1 (Eq. 10 and Eq. 11).

Error analysis

Except for comparing the determined coefficient R^2, the degree of fitting between the theoretical model and the experimental data was judged by analyzing errors. The error calculation formula of SSE is also shown in Table S1 (Eq. 16).

Results and discussion

The optimization of preparation conditions

The optimal selection of PSAC preparation conditions adopted the control variable method, and the adsorption results are shown in Table S2.

From the data in groups 1–5 in Table S2, activated carbon prepared by immersion in distilled water had a low adsorption capacity on 2,4-DCP, while the concentration of NH_4Cl had little impact on the adsorption capacity. It is likely that during the activation process, the gas generated by the decomposition of NH_4Cl can not only open the blocked channels of the activated carbon (Shen et al. 2015), but also react with its surface functional groups. That changed the surface properties of the activated carbon and improved the adsorption capacity. There is a similar phenomenon in the research of Moussavi (Moussavi et al. 2013). Overabundant NH_4Cl has no discernible impact on enhancing the adsorption capacity of activated carbon because the surface of the sample can only contact a limited amount of NH_4Cl. In this study, PSAC was prepared using NH_4Cl at a concentration of 5%.

According to the data of groups 3, 6, and 7 in Table S2, raising the activation temperature improves the prepared activated carbon's capacity to adsorb 2,4-DCP. However, the yield of activated carbon dropped from 75.2 to 43.1% when the activation temperature was raised from 673 to 773 K. The activation temperature of 673 K was determined by carefully weighing two factors.

The data in groups 3, 8, and 9 demonstrate that the yield of PSAC decreases with increasing activation time. However, when activation time rose, the activated carbon's adsorption capacity first increased slightly before declining.

The decomposition of NH_4Cl during the early stages of activation helps to increase the adsorption capacity of activated carbon, but after the decomposition of NH_4Cl is complete, further heating will destroy the pore structure and decrease the sample's specific surface area, thereby decreasing the adsorption capacity. So, 30 min were selected as the final heating period.

Characterization of adsorbent before and after activation

Comparison of adsorption capacity

The adsorption capacity of 2,4-DCP and 4-CP by PSPC was 21.9 $mg{\cdot}g^{-1}$ and 13.6 $mg{\cdot}g^{-1}$, respectively, as shown in Fig. 1. After activation, the adsorption capacity of 2,4-DCP and 4-CP by PSPC increased to 65.8 $mg{\cdot}g^{-1}$ and 45.7 $mg{\cdot}g^{-1}$, respectively. The adsorption capacity of PSAC is about three times higher than that before activation, indicating that the activation method is very effective. PSAC can be used to remove pollutants such as 2,4-DCP and 4-CP in water.

Determination of isoelectric point

Determining the isoelectric point of adsorbent is essentially determining the pH of a solution when the surface charge of the adsorbent is zero. The magnitude of the isoelectric point relies on the type and relative quantities of functional groups contained on the surface of the adsorbent.

Taking the initial pH of the solution as the horizontal coordinate, and the pH difference between the after and before the reaction, ΔpH, as the vertical ordinate, drew the chart and the point where ΔpH was zero was the isoelectric point of the adsorbent. PSAC isoelectric point determination method is the same. The results were shown in Fig. S1.

As seen from Fig. S1, the isoelectric point of PSPC is about 5.2, and the isoelectric point of PSAC is about 5.8. The reason for the isoelectric point moving to the basic range may be that the number of basic functional groups on the surface of the adsorbent increased during the activation process. When $pH < 5.8$, the surface of PSAC is positively charged so it is easy to adsorb negatively charged groups; when $pH > 5.8$, the surface of modified carbon is negatively charged so it is easy to adsorb positively charged groups.

Determination of acid–base functional groups on the surface of adsorbents

By using Boehm titration, the amounts of acidic and basic functional groups on the surfaces of PSPC and PSAC were roughly quantified (Boehm 1994). The results are presented in Table 1. It is clear that after activation, the sample's surface had more acid and basic functional groups. This result might be explained by the increased specific surface area of the adsorbent exposing more functional groups. The number of adsorption sites will climb as the number of functional

Table 1 Content of acid–base functional group

Functional group	PSPC/($mmol{\cdot}g^{-1}$)	PSAC/($mmol{\cdot}g^{-1}$)
Carboxyl group	0.3150	0.4277
Ester group	0.4044	0.5059
Phenolic hydroxyl group	0.0233	0.0600
Base functional group	0.0011	0.0114

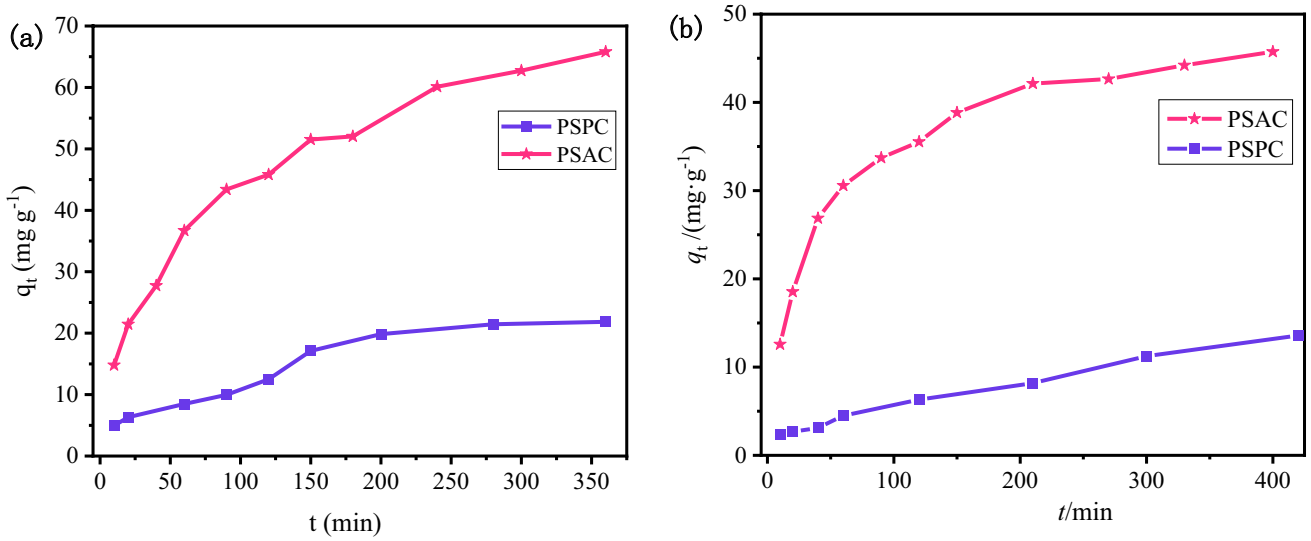

Fig. 1 Comparison of adsorption capacity of PSPC and PSAC. **a** 2,4-DCP. **b** 4-CP

groups on PSAC's surface increases, helping to raise the material's adsorption capacity.

FTIR

Fourier transform infrared (FTIR) analysis was carried out to characterize the surface organic functional groups presented on these samples. The FTIR spectrum of PSPC and PSAC is shown in Fig. S2a and S2b.

It was found from Fig. S2a and Fig. S2b that the types of functional groups contained in the adsorbent before and after activation were mainly unchanged. A strong absorption peak at about 3426 cm^{-1} was assigned to the stretching vibration of hydroxyl functional groups with hydrogen bonding. The peaks observed at 1618 and 1032 cm^{-1} could be ascribed to the stretching vibrations of C = O and C–O. The appearance of an absorption peak at about 1384 cm^{-1} indicated the presence of a $–CH_3$ group on the surfaces. And the peak at 1113 cm^{-1} probably was caused by the antisymmetric vibration of C–O–C (Gomez-Hernandez et al. 2019; Hu et al. 2021a; Jiang et al. 2010). Therefore, from FTIR analysis, it was concluded that there were hydroxyl and carboxyl groups on these activated carbon surfaces.

BET analysis

Figure S3 shows the typical adsorption/desorption isotherms of N_2 at 77 K for the PSAC, and the result for the PSPC is also shown here for a comparison purpose. The BET model was used to calculate the specific surface area.

PSPC shows a surface area value of 0.65 $m^2 \cdot g^{-1}$ which is much less than PSAC (174.87 $m^2 \cdot g^{-1}$). The PSAC prepared after activation had a significant enlargement in specific surface area, which will contribute to the improved adsorption capacity of activated carbon.

SEM

The SEM analysis was employed to gain information about the surface morphology and nature of the adsorbent before and after activation, and the results are shown in Fig. 2. PSPC had a dense structure with blocked pores, while PSAC had a loose structure with a honeycomb and well-developed pores structure. It shows that during the activation process, the gases generated by NH_4Cl decomposing filled the originally blocked channels in PSPC, making its structure fluffy, which will greatly increase the specific surface area of PSAC (Liu et al. 2018). It is also beneficial to increase the number of adsorption sites, thereby improving the adsorption capacity of PSAC. This is similar to the results of Balasubramani et. al. (2017).

XRD

The XRD patterns of PSPC and PSAC are presented in Fig. S4. Diffraction peak positions of the activated carbon before and after activation are hardly changed, suggesting that the main structure of PSPC underwent little change after being modified by NH_4Cl. Compared to the standard atlas, the pattern was in good agreement with graphite at 25° and 43°, representatives of (002) and (100) planes of graphite crystallites, which illustrates that both PSPC and PSAC might be graphitic-like structures. The activation process maintained the crystal structure of the activated carbon. Compared with PSPC, the PSAC diffraction peak intensity was slightly enhanced, which demonstrates that the activation process probably made the crystal structure of the activated carbon more ordered. Similar observations were recorded by Yang et al. in their recent study (Yang and Cannon 2021).

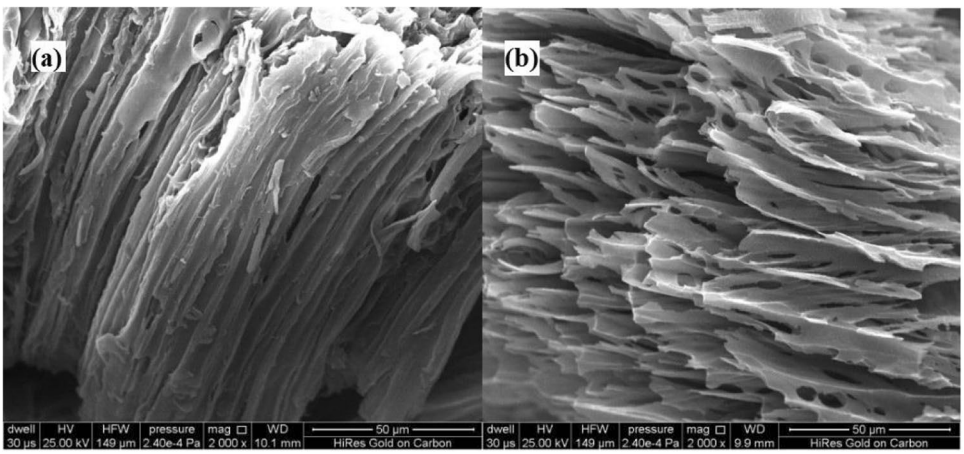

Fig. 2 SEM of PSPC (**a**) and PSAC (**b**)

Elemental composition

The content of each element in the adsorbent was determined semi-quantitatively by XRF, as shown in Table S3.

It is conspicuous from Table S3 that the content of various metal elements (such as Mg, K, Ca, and Fe) decreased after activation. It is possible that these components in the activated carbon were removed partially during activation and subsequent acid washing process. The reason for the content of Cl element increased from 0.000 to 2.390 might be that during the activation process, the –Cl generated by the decomposition of NH_4Cl was connected to the surface of PSAC. The introduction of Cl– during the pickling process may also influence the content of Cl.

The content of N, C, and H in PSPC and PSAC was determined by elemental analyzer, and the results are shown in Table S4.

Combined with the results of Boehm titration, it is speculated that during the activation process, the N caused by the decomposition of NH_4Cl reacted with the PSPC surface groups, which increased the number of basic functional groups on the surface of the sample leading to the N content in PSAC higher than that in PSPC.

Adsorption study

Effect of adsorbent dosage

In general, the adsorption behavior of PSAC for 2,4-DCP and 4-CP was similar when the amount of adsorbent was changed (Fig. S5). With the rise of the solid–liquid ratio, values of q_e gradually decreased, but values of r increased at the same condition. The adsorption capacity of PSAC for 2,4-DCP was as high as 150.1 $mg{\cdot}g^{-1}$; and the adsorption capacity for 4-CP was 58.2 $mg{\cdot}g^{-1}$. The removal efficiency of the two chlorophenols by PSAC reached more than 95%, which were 99.3% and 97.4%, respectively. This new adsorbent can well remove 2,4-DCP and 4-CP pollutants in water.

The trend of curves in Fig. S5 shows regular changes, indicating that there was no abnormal phenomenon such as adsorbent deterioration or adsorbate flocculation and coagulation when the amount of adsorbent is gradually increased. Under the experimental conditions, the obtained results can well reflect the adsorption behavior of the adsorbent. Considering the two factors of unit adsorption capacity and removal rate, in the follow-up experiments, the amount of adsorbent was kept at the solid–liquid ratio of 1.0 $g{\cdot}L^{-1}$ and 0.8 $g{\cdot}L^{-1}$, respectively.

Effect of pH

Solution pH can affect the property of adsorbent's surface and forms of adsorbate, which affect the adsorption quantity. The results are shown in Fig. 3. For 2,4-DCP (Fig. 3a), when the pH value was between about 2 and 7, q_e was mainly unchanged (about 80 $mg{\cdot}g^{-1}$). When pH continued to increase, the adsorption capacity of PSAC for 2,4-DCP decreased sharply until it was close to 0 (pH = 12). Under acid condition, 2,4-DCP is basically not ionized and appears in molecular form. Therefore, PSAC has an acceptable adsorption effect on it through intermolecular force or hydrogen bonding. As the pH value of the solution increases, the molecular state of 2,4-DCP is gradually transformed into a negative ion form due to ionization. When the pH is greater than the isoelectric point (pH = 6), the surface of the adsorbent is negatively charged. There is electrostatic repulsion between the charge and the ionized negative 2,4-DCP ions, which hinders the adsorption. This trend is same as the study by Kao et al. (Kao et al. 2000).

The effect of pH on the adsorption of 4-CP by PSAC is similar to 2,4-DCP (Fig. 3b). When pH was from 2 to 10, q_e was mainly unchanged about 50 $mg{\cdot}g^{-1}$. Subsequently, the adsorption capacity dropped sharply. The turning point of the curve in Fig. 3b is later than that in Fig. 3a, because the pK_a value of 4-CP (pK_a = 9.38) (Dan et al. 2021) is larger than that of 2,4-DCP (pK_a = 7.85) (Han et al. 2010), and ionization can only occur at a higher pH value.

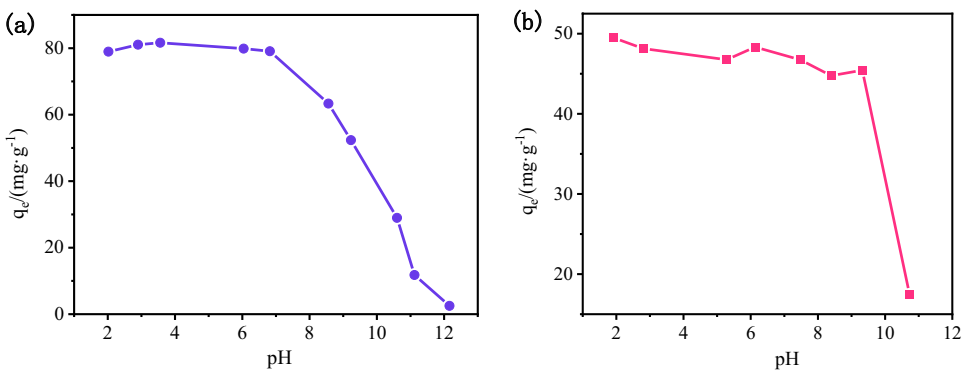

Fig. 3 The influence of pH on 2,4-DCP (**a**) and 4-CP (**b**) adsorptions on PSAC

Effect of salt concentration

It is well known that industrial wastewater contains other pollutants, especially salts. It is necessary to study the effect of some common salts on the adsorption process in order to evaluate the practical application of adsorbents. The choice for these salts was based on the premise that they can be used as a model for studying the competitive effect of monovalent and divalent cations on the adsorption process (Aryee et al. 2020) Therefore, chose two common salts (NaCl and Na_2SO_4) to analyze the effect of ions concentration. The presence of inorganic salts had little influence on the ability of PSAC to adsorb 2,4-DCP and 4-CP (Fig. S6a and 6b). Despite an increase in salt concentration, the equilibrium adsorption capacity of PSAC remained relatively unchanged. Inorganic salt ions can reduce the electric double layer's thickness on PSAC's surface and lessen the electrostatic attraction between PSAC and chlorophenol, which is detrimental to the electrostatic adsorption process (Wang et al. 2022b). On the other hand, lowering 2,4-DCP and 4-CP solubility in water is conducive to adsorption. As was already indicated, we deduce that intermolecular forces, particularly hydrogen bonds, may play a major role in the adsorption of 2,4-DCP and 4-CP by PSAC. So, the presence of inorganic salts may have little impact.

Effects of equilibrium concentration and temperature on adsorption and isotherm

Adsorption of 2,4-DCP (or 4-CP) onto 10 mg (8 mg) of PSAC was studied using different concentrations of adsorbate at 293, 303, and 313 K. The variation of adsorption capacity (q_e) with concentration at equilibrium (C_e), namely adsorption isotherm, is presented in Fig. 4. The value of adsorption capacity was gradually increased as the concentration of adsorbate solution increased.

The effect of temperature on the adsorption of 2,4-DCP by PSAC is more distinct than that on 4-CP. At the same equilibrium concentration, q_e of 2,4-DCP increased significantly with the increase of temperature, indicating that the adsorption process is the endothermic reaction (Fig. 4a). It can be seen from Fig. 4b that the adsorption amount of 4-CP by PSAC increases slightly with the increase of temperature. So, the effect of temperature is not insignificant for the adsorption of 4-CP onto PSAC.

Four models, including Langmuir, Freundlich, Temkin, and Koble-Corrigan models, were used to perform nonlinear fitting on the adsorption 2,4-DCP isotherm of PSAC, and SSE error analysis was done on the fitting results. The results are listed in Table 2 and the fitted curves are also shown in Fig. 4a. It was found that that the R^2 values of the four models descend in the order: Freundlich > Koble-Corrigan > Temkin > Langmuir.

The maximum unit adsorption quantity obtained by fitting the model is consistent with the experimental value, even though $R^2 < 0.9$ and the error analysis is rather considerable. It implies that the 2,4-DCP adsorption by PSAC is not an ideal monolayer adsorption process, but there could be a step in the overall adsorption process that is better suited for monolayer adsorption (Zhou et al. 2019).

The Freundlich model, an empirical equation under non-ideal conditions, is used to describe the adsorption process of multi-molecular layers on non-uniform surfaces. The parameter $1/n$ in the model represents the adsorption strength of the adsorbent, which is related to the degree of inhomogeneity (Mpatani et al. 2020b). The surface of the adsorbent is more uneven, and the value of $1/n$ is within the range of 0.235 ~ 0.312 (Chowdhury et al. 2011). This indicates that the adsorption of 2,4-DCP by PSAC is easy to carry out, and the adsorption process is multi-molecular layer adsorption on a non-uniform surface.

The Koble-Corrigan model isotherm correlates the adsorption data with R^2 value of 0.991 demonstrating the heterogeneous surface adsorption of 2,4-DCP on PSAC. The Koble-Corrigan model is a three-parameter equation and a combination of the Langmuir model and the Freundlich model. When $n = 1$, the Koble-Corrigan equation is transformed to the shape of Langmuir. And when $B = 0$ in the model, the equation is converted into the Freundlich form (Zheng et al. 2015). Based on Table 2, the

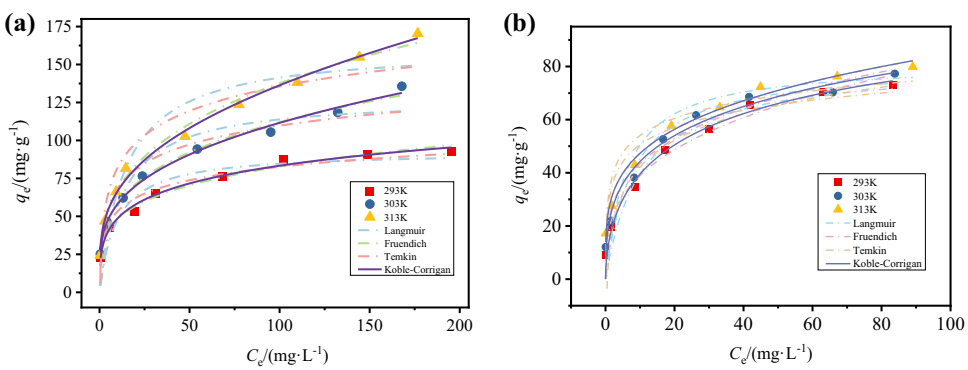

Fig. 4 Adsorption isotherms of 2,4-DCP (**a**) and 4-CP (**b**) onto PSAC

Table 2 Parameters of the isotherms and error results of 2,4-DCP and 4-CP adsorption

Parameters	2,4-DCP			4-CP		
	293 K	303 K	313 K	293 K	303 K	313 K
Langmuir						
K_L/(L·mg^{-1})	0.106	0.079	0.070	0.096	0.128	0.164
$q_{m(exp)}$/(mg·g^{-1})	92.8	135.7	170.4	73.2	77.3	79.9
$q_{m(theo)}$/(mg·g^{-1})	92.6	128.2	161.4	80.6	80.6	81.1
R^2	0.876	0.883	0.903	0.955	0.943	0.894
SSE	550.9	1152.9	1942.0	178.6	228.1	404.6
Freundlich						
K_F	28.11	30.50	32.75	18.6	22.8	26.6
1/*n*	0.235	0.283	0.312	0.320	0.280	0.251
R^2	0.987	0.992	0.993	0.967	0.978	0.987
SSE	55.9	74.5	142.6	130.7	86.7	49.2
Temkin						
A	23.79	27.21	28.46	9.01	29.1	32.5
B	12.78	17.92	23.26	14.4	9.34	9.35
R^2	0.965	0.931	0.924	0.965	0.894	0.905
SSE	155.9	681.6	1530.6	54.7	425.3	359.6
Koble-Corrigan						
A	29.09	29.01	31.29	16.1	23.7	26.4
B	0.122	−0.103	−0.125	0.131	0.122	−0.008
n	0.322	0.220	0.225	0.556	0.384	0.247
R^2	0.991	0.994	0.995	0.974	0.981	0.987
SSE	41.71	62.72	101.8	102.5	74.9	49.1

Koble-Corrigan model can well describe the adsorption process of 2,4-DCP by PSAC. The model parameters-*n* are all less than 0.5, and *B* is close to 0, indicating that the model is more inclined to the Freundlich form, which further proves that the adsorption of 2,4-DCP by PSAC is non-uniform surface adsorption.

For the isotherm of PSAC adsorption of 4-CP (Fig. 4b), the adsorption of 4-CP by PSAC is relatively consistent with the Freundlich ($R^2 > 0.96$) and Koble-Corrigan ($R^2 > 0.97$) models. The parameter 1/*n* in the Freundlich model is 0.251 to 0.320, indicating that the adsorption is accessible to carry out. Like the adsorption process of 2,4-DCP, the adsorption of 4-CP by PSAC is also heterogeneous surface adsorption.

The theoretical maximum unit adsorption quantity of PSAC for 2,4-DCP and 4-CP were 135.7 and 77.3 mg·g^{-1}. Table 3 lists the comparison of the maximum adsorption capacity of various types of 2,4-DCP and 4-CP on various adsorbents. The adsorption capacity of PSAC for 2,4-DCP and 4-CP was relatively high and comparable to some previous works reported in the literature. As can be seen from the data listed in Table 3, although the theoretical maximum adsorption capacity of some materials is greater than that of PSAC, PSAC is a promising material for its application due to its low cost and simple preparation process. So, there is some advantage for PSAC to remove some pollutants.

Effect of contact time and kinetic studies

Experimental kinetics data for PSAC adsorption at different initial concentrations were plotted as adsorbed amounts versus contact time, as shown in Fig. 5. Significantly, absorption of both adsorbates appeared to be rapid at first, with much of the adsorbate concentration removed in the first 100 min. Thereafter, it becomes slowly increased until the equilibrium. The fast adsorption at the initial stage may be attributed to the higher driving force making fast transfer of adsorbate to the surface of carbon particles and the availability of the uncovered surface area and the remaining active sites on the adsorbent (Okolo et al. 2000).

As shown in Fig. 5a, the adsorption kinetics curves of PSAC to 2,4-DCP have the same trend with temperature under different adsorbate concentrations. When the initial concentration of 2,4-DCP is 75 mg·L^{-1}, the equilibrium adsorption capacities of PSAC were 48.1 mg·g^{-1} (293 K), 53.9 mg·g^{-1} (303 K), and 62.9 mg·g^{-1} (313 K), respectively. With the increase in temperature, the adsorption speed became faster, and the equilibrium adsorption capacity increased. It is indicated that the adsorption reaction is an endothermic process, which is the same as the results obtained from the adsorption isotherms at different temperatures. With the increase of adsorbate (Fig. 5b), the values of adsorption quantity became larger.

Table 3 Comparison of maximum adsorption capacities for 2,4-DCP and 4-CP removal using different adsorbents

Adsorbate	Adsorbent	q_m/(mg·g^{-1})	*t*/min	pH	*T*/K	Advantage	Disadvantage	Ref.
2,4-DCP	Fe_3O_4@AC–SS	98.04	60	5–7	298	Magnetic separation; short adsorption time; non-toxic	Expensive; inconvenient preparation process	(Gopal et al. 2019)
2,4-DCP	CPC-PS	71.40	180	2–8	298	Economic; waste recycling	Normal adsorption performance	(Wang et al. 2022b)
2,4-DCP	GN	242.72	700	3–6	298	Excellent adsorption performance	Inconvenient preparation process; long adsorption time	(Liu et al. 2020)
2,4-DCP	HCPC	306.75	700	3–6	298			(Liu et al. 2020)
2,4-DCP	GN/HCPC	348.43	700	3–6	298			(Liu et al. 2020)
2,4-DCP	ZIF-8	107.07	240	7–10	323	Alkaline condition adsorption	Expensive; inconvenient preparation process	(Wang et al. 2021a)
2,4-DCP	PANI/BH	43.48	120	7	303	Short adsorption time; waste recycling	Poor adsorption performance	(Bhatti et al. 2020)
2,4-DCP	GP/MIL-53(Cr)	98.20	40	6–10	301	Excellent recyclability	Toxic heavy metal ions; time-consuming preparation process	(Oni and Sanni 2022)
2,4-DCP	PSAC	135.7	300	2–7	303	Economic; waste recycling, eco-friendly		This work
4-CP	MWCNT	111.11	-	5–7	303		Normal recyclability	(Madannejad et al. 2018)
4-CP	SWCNT	58.83	-	5–7	303			(Madannejad et al. 2018)
4-CP	CSAC	72.8	150	2–4	303	Excellent recyclability; simple synthesis; low cost		(Radhika and Palanivelu 2006)
4-CP	Surfactant-modified zeolite	12.7	30	-	293	Natural adsorbent;	Poor adsorption performance	(Kuleyin 2007)
4-CP	PSAC	77.3	450	2–10	303	Economic; waste recycling, eco-friendly		This work

From Fig. 5c, with the increase of temperature, the adsorption speed of PSAC on the adsorption of 4-CP became faster. At 293, 303, and 313 K, the equilibrium adsorption capacities of PSAC were 44.1, 44.9 mg·g^{-1}, and 45.6 mg·g^{-1}, respectively. And the equilibrium adsorption capacities did not change significantly at different temperatures. This is consistent with the results obtained from the isotherm, indicating that the temperature factor has little effect on the ability of PSAC to adsorb 4-CP.

Additionally, increasing the adsorbate concentration may accelerate the adsorption rate of the adsorbent. But the equilibrium adsorption quantities of the adsorbent also increase, and it takes longer time to reach the adsorption equilibrium (Fig. 5d).

Three models, including pseudo-second-order kinetics, Elovich, and intraparticle diffusion, were used to nonlinearly correlate the kinetic curve of PSAC adsorption of 2,4-DCP. The fitted analysis results such as SSE are shown in Table 4 and the fitted curves are also presented in Fig. 5.

The pseudo-second-order kinetic model can describe the adsorption of 2,4-DCP by PSAC adequately. The values of R^2 were all above 0.948, and error values were relatively small. Values of q_e obtained from the pseudo-second-order kinetic model were also similar to the experimental values. This suggested that chemisorption, which was accompanied by the sharing or exchange of electrons between the adsorbent and the adsorbate as well as the breakdown or creation of chemical bonds, may be the rate-controlling stage in the PSAC adsorption process (Shaarani and Hameed 2011).

In addition to the pseudo-second-order kinetic model, the adsorption of 2,4-DCP onto PSAC was also in line with the Elovich model based the values of R^2 (> 0.970) and SSE (< 42.3).

Value of *C*, one parameter linked to the thickness of the boundary layer, is not equal to zero in Table 4, showing that there is some boundary layer diffusion occurring throughout the adsorption process and that intra-particle diffusion is not the only rate-controlling activity. It is generally believed that the larger the value of *C*, the greater the influence of the boundary layer (Khenifi et al. 2009). Additionally, *C* increases with the rise of temperature and the initial concentration of 2,4-DCP. That illustrates that the higher the

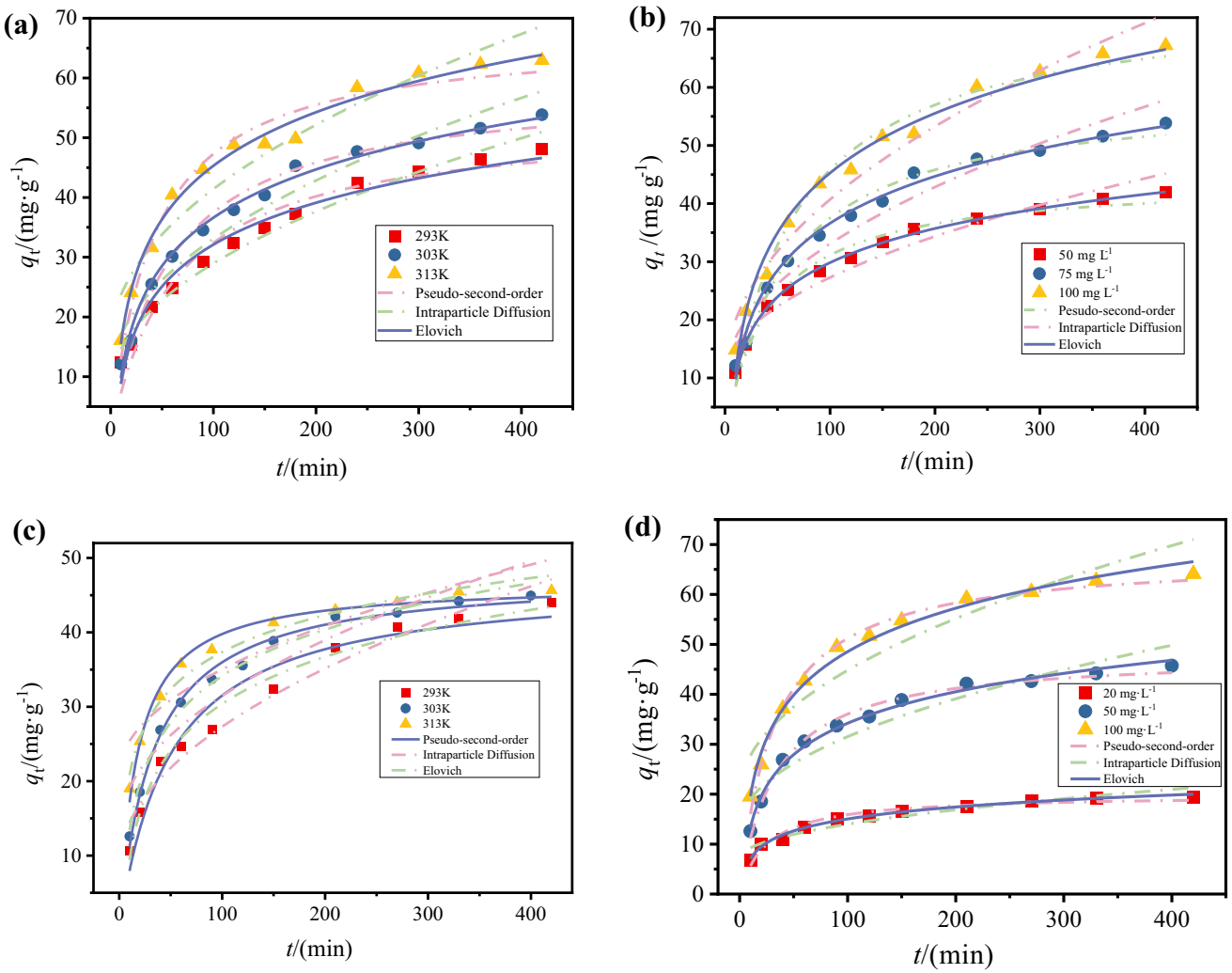

Fig. 5 Effect of contact time on adsorption at $C_0 = 75$ mg L^{-1} for 2,4-DCP (**a**) and 50 mg L^{-1} for 4-CP (**c**) at different temperatures. Effect of contact time on adsorption at different concentration for 2,4-DCP (**b**) and 4-CP (**d**) at 303 K

adsorption reaction temperature and adsorbate concentration is, the greater effect of boundary layer diffusion on the adsorption rate is.

The fitting results of the adsorption kinetic curve model of PSAC on 4-CP are shown in Table 5. Based on the values of R^2 and SSE, the pseudo-second-order kinetic model and Elovich equation can describe the adsorption system adequately. Furthermore, the fitted curves from both models were closer to experimental points. The values of q_e from the second-order kinetic model were also close to the experimental values. This implied that this model can predict the equilibrium adsorption quantity.

According to the kinetic model fitted to the adsorption behavior of 4-CP by PSAC, it can be inferred that the adsorption process may contain chemisorption. In the intra-particle diffusion model, the constant C is not zero, indicating that the intra-particle diffusion is not an only speed-controlled factor in the adsorption process. The adsorption of 2,4-DCP and 4-CP by PSAC, whose the kinetic curves are in good agreement with the pseudo-second-order kinetic model and the Elovich equation, has a similar mechanism.

Thermodynamic parameters and apparent activation energy

By calculating the thermodynamic parameters and apparent activation energy, the adsorption reaction mechanism can be further understood. According to Eq. S13-15, ΔH, ΔS, ΔG, and apparent activation energy E_a during the adsorption of 2,4-DCP and 4-CP by PSAC were calculated, respectively. The results are shown in Table 6.

According to the equations $\Delta H > 0$, $\Delta S > 0$, and $\Delta G < 0$, the adsorptions of 2,4-DCP and 4-CP by PSAC are both spontaneous endothermic reactions, and the entropy

Table 4 Parameters of the kinetic models and error result of 2,4-DCP adsorption

Pseudo–second–order equation						
T/K	C_0/(mg·L^{-1})	$q_{e(exp)}$/(mg·g^{-1})	k_2/(g·mg^{-1}·min^{-1})	$q_{e(theo)}$/(mg·g^{-1})	R^2	SSE
293	75	48.1	2.98E-04	52.9	0.962	60.4
303	50	42.0	5.36E-04	44.2	0.979	22.5
303	75	53.9	2.98E-04	58.9	0.986	29.7
303	100	67.2	2.05E-04	75.4	0.980	68.2
313	75	62.9	3.54E-04	67.2	0.974	67.2
Elovich equation						
T/K	C_0/(mg·L^{-1})	$q_{e(exp)}$/(mg·g^{-1})	α	β	R^2	SSE
293	75	48.1	2.41	0.099	0.978	34.5
303	50	42.0	2.86	0.118	0.998	2.42
303	75	53.9	2.69	0.086	0.992	15.9
303	100	67.2	3.14	0.067	0.986	46.3
313	75	62.9	4.28	0.077	0.990	26.7
Intraparticle diffusion						
T/K	C_0/(mg·L^{-1})	$q_{e(exp)}$/(mg·g^{-1})	K_t	C	R^2	SSE
293	75	48.1	2.10	7.96	0.981	30.4
303	50	42.0	1.70	10.2	0.940	65.8
303	75	53.9	2.36	9.47	0.948	108.1
303	100	67.2	3.03	10.4	0.963	124.7
313	75	62.9	2.60	15.4	0.928	184.8

Table 5 Parameters of the kinetic models and error results of 4-CP adsorption

Pseudo–second–order equation						
T/K	C_0/(mg·L^{-1})	$q_{e(exp)}$/(mg·g^{-1})	k_2/(g·mg^{-1} min^{-1})	$q_{e(theo)}$/(mg·g^{-1})	R^2	SSE
293	50	44.1	4.31E-04	47.0	0.964	42.7
303	50	44.9	6.41E-04	47.7	0.991	10.3
313	50	45.6	1.25E-03	46.6	0.987	9.74
303	20	19.5	1.99E-03	19.9	0.959	7.09
303	100	64.1	4.58E-04	67.7	0.991	20.5
Elovich equation						
T/K	C_0/(mg·L^{-1})	$q_{e(exp)}$/(mg·g^{-1})	α	β	R^2	SSE
293	50	44.1	2.56	0.110	0.987	15.0
303	50	44.9	3.99	0.111	0.991	10.6
313	50	45.6	13.0	0.139	0.980	15.2
303	20	19.5	2.67	0.289	0.990	1.74
303	100	64.1	6.00	0.080	0.990	22.0
Intraparticle diffusion						
T/K	C_0/(mg·L^{-1})	$q_{e(exp)}$/(mg·g^{-1})	K_t	C	R^2	SSE
293	50	44.1	1.89	8.40	0.966	40.1
303	50	44.9	1.81	13.4	0.892	124.1
313	50	45.6	1.41	20.9	0.859	104.9
303	20	19.5	0.70	7.00	0.912	15.1
303	100	64.1	2.50	19.8	0.891	246.8

Table 6 Thermodynamic data obtained from adsorption of 2,4-DCP and 4-CP on PSAC

	E_a/(kJ·mol^{-1})	ΔH/(kJ·mol^{-1})	ΔS/(J·mol^{-1}·K^{-1})	ΔG/(kJ·mol^{-1})		
				293 K	303 K	313 K
2,4-DCP	9.59	23.6	108.1	− 8.02	− 9.27	− 10.2
4-CP	40.5	18.1	94.0	− 9.39	− 10.5	− 11.3

increases during the adsorption process. It is widely believed that when $\Delta H < 84$ kJ·mol^{-1} or $5 < E_a < 40$ kJ·mol^{-1}, the adsorption process is a physical adsorption; when $84 < \Delta H < 420$ kJ·mol^{-1} or $E_a > 40$ kJ·mol^{-1}, the adsorption process is a chemical adsorption (Hu and Han 2019). As a result, the adsorption of 2,4-DCP by PSAC is physical adsorption, and the adsorption of 4-CP by PSAC contains both physical adsorption and chemical adsorption. Considering that the kinetic curves of PSAC adsorption of 2,4-DCP and 4-CP are suitable with the pseudo-second-order kinetic model, the adsorption process of PSAC to the two chlorophenols may be both chemical adsorption and physical adsorption.

Desorption/regeneration studies

The potential of spent adsorbents can be regenerated and applied for further use, and this can make the process economical and cost-effective (Bhatti et al. 2020; Dovi et al. 2022; Wang et al. 2021b). Figure 6a and b display the results of different methods to desorb PSAC. Eighty percent of ethanol was used to conduct multiple regeneration experiments to study the reproducibility of PSAC adsorbed 2,4-DCP. The desorption rate and regeneration rate after three desorption regeneration are shown in Fig. 6c. With the increase of regeneration times, the desorption rate and regeneration rate of PSAC gradually decrease, but the decrease range is small. And the third regeneration rate is about 68%. The adsorption capacity of PSAC to 2,4-DCP becomes smaller after repeated regeneration, but it can be recycled within a limited number of times.

Fifty percent of ethanol was used to conduct multiple regeneration experiments to study the regeneration ability of PSAC after adsorbing 4-CP. The results of three consecutive regenerations are shown in Fig. 6d. The three regenerations have good effects, and the desorption rate and regeneration rate are about 70% and 80%, respectively. After multiple regenerations of PSAC, the adsorption capacity of 4-CP did not decrease significantly, indicating that PSAC could be regenerated and recycled after adsorbing 4-CP.

The plausible mechanism of adsorption

The adsorption of 2,4-DCP and 4-CP by PSAC has a relatively similar mechanism. According to the effects of pH and coexisting ion, salinity has almost no effect on the adsorption. When pH < p*K*a, 2,4-DCP and 4-CP appear in molecular form, indicating that PSAC has a good adsorption of these two chlorophenolic compounds through intermolecular forces or hydrogen bonding, etc. The Freundlich model can well describe the adsorption of PSAC on 2,4-DCP and 4-CP adsorption, indicating that the adsorption process is multimolecular layer adsorption on inhomogeneous surfaces. The results of kinetic and thermodynamic analyses investigated

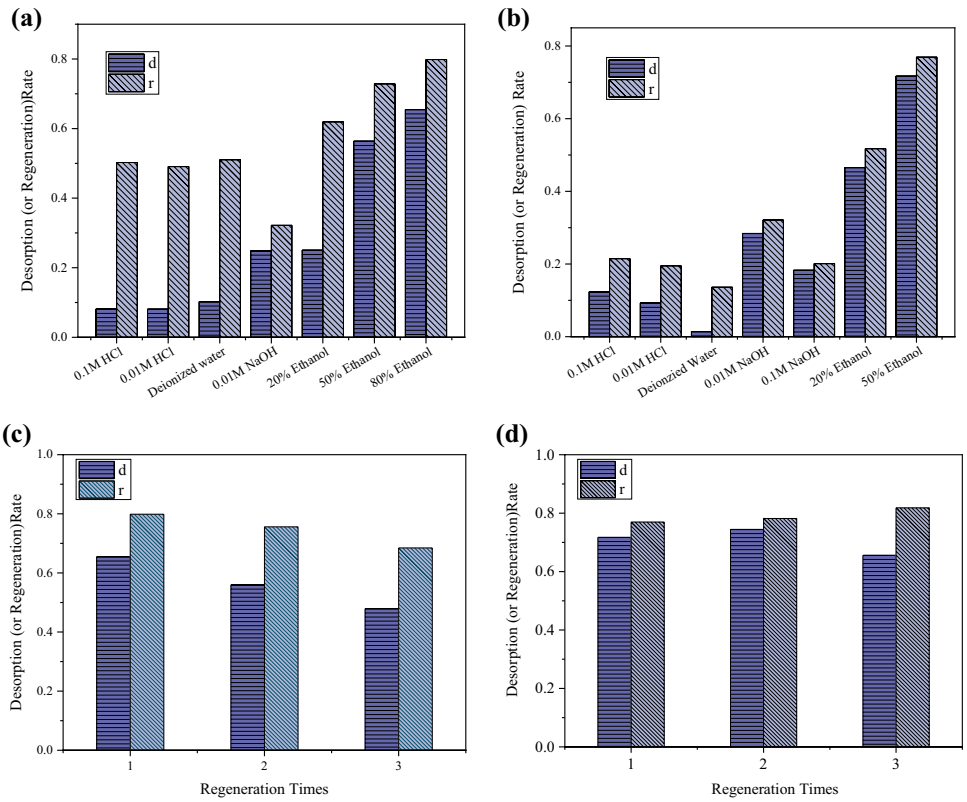

Fig. 6 Different desorption methods of PSAC for 2,4-DCP (**a**) and 4-CP (**b**). Multiple regenerations after PSAC adsorption of 2,4-DCP (**c**) and 4-CP (**d**)

the simultaneous physical and chemical adsorption of PSAC on the two chlorophenolic compounds.

Conclusion

The adsorption performance of PSAC prepared by NH_4Cl activation to 2,4-DCP and 4-CP was obviously improved. The acidic conditions are favorable for the adsorption of 2,4-DCP and 4-CP by PSAC. The phenolic hydroxyl groups become negatively charged as the pH value rises, which can prevent adsorption owing to electrostatic repulsion. Furthermore, the salinity has only a minor impact on this adsorption process. The Freundlich and Koble-Corrigan models exhibit good agreement with the 2,4-DCP and 4-CP adsorption while the adsorption process can be properly described by the pseudo-second-order kinetic model and Elovich equation, demonstrating the presence of chemical adsorption in the adsorption process. The processes of 2,4-DCP and 4-CP adsorption are both spontaneous endothermic processes, and physical adsorption occurs during the adsorption process. Comprehensively, both physical adsorption and chemical adsorption exist in the process of PSAC adsorption of two chlorophenols. Ethanol can be used to regenerate PSAC adsorbed of 2,4-DCP and 4-CP.

In order to make the adsorbent can be applied in practice, it is necessary to further study the effect of adsorbent on the actual wastewater treatment. In order to make full use of the adsorbent and reduce the cost, the regeneration method can be further investigated to find a better, cheaper, and secondary pollution-free treatment method. Alternatively, the adsorption effect of PSAC on other pollutants can be studied to expand the application of adsorbents. Promisingly, PSAC is hereby presented as an adsorbent from a low/no cost industrial residue that is promising for application in the control of water pollution and presents a very valuable economic with benefits to the environment.

Supplementary Information The online version contains supplementary material available at https://doi.org/10.1007/s11356-022-24403-9.

Author contribution Yuwei Song: conceptualization; methodology; formal analysis; investigation; visualization, software; writing original draft.

Yuanyuan Wang: software, writing-review and editing, formal analysis.

Runping Han: conceptualization; resources; project administration; writing—review and editing; visualization; supervision; funding acquisition.

Funding This work was financially supported by the Henan province basis and advancing technology research project (142300410224).

Data availability All data generated or analyzed during this study are included in this published article.

Declarations

Ethics approval Not applicable.

Consent to participate Not applicable.

Consent for publication Not applicable.

Competing interests The authors declare no competing interests.

References

Ahmed MJ, Theydan SK (2013) Adsorption of p-chlorophenol onto microporous activated carbon from Albizia lebbeck seed pods by one-step microwave assisted activation. J Anal Appl Pyrolysis 100:253–260. https://doi.org/10.1016/j.jaap.2013.01.008

Aryee AA, Mpatani FM, Kani AN, Dovi E, Han RP, Li ZH, Qu LB (2020) Iminodiacetic acid functionalized magnetic peanut husk for the removal of methylene blue from solution: characterization and equilibrium studies. Environ Sci Pollut Res 27:40316–40330. https://doi.org/10.1007/s11356-020-10087-6

Balasubramani U, Venkatesh R, Subramaniam S, Gopalakrishnan G, Sundararajan V (2017) Alumina/activated carbon nano-composites: synthesis and application in sulphide ion removal from water. J Hazard Mater 340:241–252. https://doi.org/10.1016/j.jhazmat.2017.07.006

Bhatti HN, Mahmood Z, Kausar A, Yakout SM, Shair OH, Iqbal M (2020) Biocomposites of polypyrrole, polyaniline and sodium alginate with cellulosic biomass: adsorption-desorption, kinetics and thermodynamic studies for the removal of 2,4-dichlorophenol. Int J Biol Macromol 153:146–157. https://doi.org/10.1016/j.ijbiomac.2020.02.306

Boehm HP (1994) Some aspects of the surface-chemistry of carbon-blacks and other carbons. Carbon 32:759–769. https://doi.org/10.1016/0008-6223(94)90031-0

Chen XY, Hossain MF, Duan CY, Lu J, Tsang YF, Islam MS, Yanbo Zhou YB (2022) Isotherm models for adsorption of heavy metals from water—a review. Chemosphere 307:135545. https://doi.org/10.1016/j.chemosphere.2022.135545

Chowdhury S, Mishra R, Saha P, Kushwaha P (2011) Adsorption thermodynamics, kinetics and isosteric heat of adsorption of malachite green onto chemically modified rice husk. Desalination 265:159–168. https://doi.org/10.1016/j.desal.2010.07.047

Dan XW, Luo ZY, Dai M, Zhang M, Yue X, Xie SL (2021) Oxidative degradation of p-chlorophenol by ferrate(VI): kinetics, intermediates and pathways. J Environ Chem Eng 9:105810. https://doi.org/10.1016/j.jece.2021.105810

De Castro M, Abad MLB, Sumalinog DAG, Abarca RRM, Paoprasert P, de Luna MDG (2018) Adsorption of methylene blue dye and Cu(II) ions on EDTA-modified bentonite: isotherm, kinetic and thermodynamic studies. Sustain Environ Res 28:197–205. https://doi.org/10.1016/j.serj.2018.04.001

Dovi E, Aryee AA, Li JJ, Li ZH, Qu LB, Han RP (2022) Amine-grafted walnut shell for efficient removal of phosphate and nitrate. Environ Sci Pollut Res 29:20976–20995. https://doi.org/10.1007/s11356-021-16963-z

Duan CY, Ma TY, Wang JY, Zhou YB (2020) Removal of heavy metals from aqueous solution using carbon-based adsorbents: a review. J Water Process Eng 37:101339. https://doi.org/10.1016/j.jwpe.2020.101339

Fang LP, Xu CH, Zhang WB, Huang LZ (2018) The important role of polyvinylpyrrolidone and Cu on enhancing dechlorination of 2,4-dichlorophenol by Cu/Fe nanoparticles: performance and

mechanism study. Appl Surf Sci 435:55–64. https://doi.org/10.1016/j.apsusc.2017.11.084
Garba ZN, Zhou WM, Lawan I, Xiao W, Zhang MX, Wang LW, Chen LH, Yuan ZH (2019) An overview of chlorophenols as contaminants and their removal from wastewater by adsorption: a review. J Environ Manage 241:59–75. https://doi.org/10.1016/j.jenvman.2019.04.004
Ghaffari A, Tehrani MS, Husain SW, Anbia M, Azar PA (2014) Adsorption of chlorophenols from aqueous solution over amino-modified ordered nanoporous silica materials. J Nanostruct Chem 4:114. https://doi.org/10.1007/s40097-014-0114-1
Gomez-Hernandez R, Panecatl-Bernal Y, Mendez-Rojas MA (2019) High yield and simple one-step production of carbon black nanoparticles from waste tires. Heliyon 5:e02139. https://doi.org/10.1016/j.heliyon.2019.e02139
Gopal K, Mohd NI, Raoov M, Suah FBM, Yahaya N, Zain NNM (2019) Development of a new efficient and economical magnetic sorbent silicone surfactant-based activated carbon for the removal of chloro- and nitro-group phenolic compounds from contaminated water samples. RSC Adv 9:36915–36930. https://doi.org/10.1039/c9ra07151b
Han DM, Jia WP, Liang HD (2010) Selective removal of 2,4-dichlorophenoxyacetic acid from water by molecularly-imprinted amino-functionalized silica gel sorbent. J Environ Sci 22:237–241. https://doi.org/10.1016/s1001-0742(09)60099-1
Hu BT, Gu ZL, Su JW, Li ZJ (2021) Pyrolytic characteristics and kinetics of Guanzhong wheat straw and its components for high-value products. Bioresources 16:1958–1979. https://doi.org/10.15376/biores.16.1.1958-1979
Hu HT, Miao KK, Luo XL, Guo SF, Yuan XQ, Pei F, Qian HM, Feng GD (2021b) Efficient Fenton-like treatment of high-concentration chlorophenol wastewater catalysed by Cu-Doped SBA-15 mesoporous silica. J Clean Prod 318:128632. https://doi.org/10.1016/j.jclepro.2021.128632
Hu YY, Han RP (2019) Selective and efficient removal of anionic dyes from solution by zirconium(IV) hydroxide-coated magnetic materials. J Chem Eng Data 64:791–799. https://doi.org/10.1021/acs.jced.8b01063
Jiang XX, Ellis N, Zhong ZP (2010) Characterization of pyrolytic lignin extracted from bio-oil. Chin J Chem Eng 18:1018–1022. https://doi.org/10.1016/s1004-9541(09)60162-2
Kao PC, Tzeng JH, Huang TL (2000) Removal of chlorophenols from aqueous solution by fly ash. J Hazard Mater 76:237–249. https://doi.org/10.1016/s0304-3894(00)00201-6
Khenifi A, Zohra B, Kahina B, Houari H, Zoubir D (2009) Removal of 2,4-DCP from wastewater by CTAB/bentonite using one-step and two-step methods: a comparative study. Chem Eng J 146:345–354. https://doi.org/10.1016/j.cej.2008.06.028
Kuleyin A (2007) Removal of phenol and 4-chlorophenol by surfactant-modified natural zeolite. J Hazard Mater 144:307–315. https://doi.org/10.1016/j.jhazmat.2006.10.036
Liu X, Wan YB, Liu PL, Fu YZ, Zou WH (2018) A novel activated carbon prepared from grapefruit peel and its application in removal of phenolic compounds. Water Sci Technol 77:2517–2527. https://doi.org/10.2166/wst.2018.212
Liu YY, Men B, Hu AB, You QL, Liao GY, Wang DS (2020) Facile synthesis of graphene-based hyper-cross-linked porous carbon composite with superior adsorption capability for chlorophenols. J Environ Scis 90:395–407. https://doi.org/10.1016/j.jes.2019.11.018
Madannejad S, Rashidi A, Sadeghhassani S, Shemirani F, Ghasemy E (2018) Removal of 4-chlorophenol from water using different carbon nanostructures: a comparison study. J Mol Liq 249:877–885. https://doi.org/10.1016/j.molliq.2017.11.089
Mallakpour S, Sirous F, Hussain CM (2021) Sawdust, a versatile, inexpensive, readily available bio-waste: from mother earth to valuable materials for sustainable remediation technologies. Adv Colloid Interface Sci 295:102492. https://doi.org/10.1016/j.cis.2021.102492
Mannai I, Sayen S, Arfaoui A, Touil A, Guillon E (2022) Copper removal from aqueous solution using raw pine sawdust, olive pomace and their derived traditional biochars. Int J Environ Sci Technol 19:6981–6992. https://doi.org/10.1007/s13762-021-03629-z
Moussavi G, Alahabadi A, Yaghmaeian K, Eskandari M (2013) Preparation, characterization and adsorption potential of the NH_4Cl-induced activated carbon for the removal of amoxicillin antibiotic from water. Chem Eng J 217:119–128. https://doi.org/10.1016/j.cej.2012.11.069
Mpatani FM, Aryee AA, Kani AN, Guo QH, Dovi E, Qu LB, Li ZH, Han RP (2020a) Uptake of micropollutant-bisphenol A, methylene blue and neutral red onto a novel bagasse-beta-cyclodextrin polymer by adsorption process. Chemosphere 259:127439. https://doi.org/10.1016/j.chemosphere.2020.127439
Mpatani FM, Aryee AA, Kani AN, Wen K, Dovi E, Qu L, Li Z, Han R (2020b) Removal of methylene blue from aqueous medium by citrate modified bagasse: kinetic, equilibrium and thermodynamic study. Bioresour Technol Rep 11:100463. https://doi.org/10.1016/j.biteb.2020.100463
Nasser A, Mingelgrin U (2014) Birnessite-induced mechanochemical degradation of 2,4-dichlorophenol. Chemosphere 107:175–179. https://doi.org/10.1016/j.chemosphere.2013.11.058
Okolo B, Park C, Keane MA (2000) Interaction of phenol and chlorophenols with activated carbon and synthetic zeolites in aqueous media. J Colloid Interface Sci 226:308–317. https://doi.org/10.1006/jcis.2000.6796
Oni BA, Sanni SE (2022) Cationic graphene-based polymer composite modified with chromium-based metal-organic framework GP/MIL-53(Cr) for the degradation of 2,4-dichlorophenol in aqueous solution. Mater Today Sustain 18:100134. https://doi.org/10.1016/j.mtsust.2022.100134
Ozacar M, Sengil IA (2005) Adsorption of metal complex dyes from aqueous solutions by pine sawdust. Bioresour Technol 96:791–795. https://doi.org/10.1016/j.biortech.2004.07.011
Quan XC, Shi HC, Liu H, Lv PP, Qian Y (2004) Enhancement of 2,4-dichlorophenol degradation in conventional activated sludge systems bioaugmented with mixed special culture. Water Res 38:245–253. https://doi.org/10.1016/j.watres.2003.09.003
Radhika M, Palanivelu K (2006) Adsorptive removal of chlorophenols from aqueous solution by low cost adsorbent—kinetics and isotherm analysis. J Hazard Mater 138:116–124. https://doi.org/10.1016/j.jhazmat.2006.05.045
Ramos-Ramirez E, Gutierrez-Ortega NL, Tzompantzi-Morales F, Barrera-Rodriguez A, Castillo-Rodriguez JC, Tzompantzi-Flores C, Santolalla-Vargas CE, Guevara-Hornedo MD (2020) Photocatalytic degradation of 2,4-Dichlorophenol on NiAl-mixed oxides derivatives of activated layered double hydroxides. Top Catal 63:546–563. https://doi.org/10.1007/s11244-020-01269-0
Shaarani FW, Hameed BH (2011) Ammonia-modified activated carbon for the adsorption of 2,4-dichlorophenol. Chem Eng J 169:180–185. https://doi.org/10.1016/j.cej.2011.03.002
Shen BX, Li GL, Wang FM, Wang YY, He C, Zhang M, Singh S (2015) Elemental mercury removal by the modified bio-char from medicinal residues. Chem Eng J 272:28–37. https://doi.org/10.1016/j.cej.2015.03.006
Sun YF, Liu ZT, Fei ZH, Li CS, Chun Y, Zhang AM (2019) Synergistic effect and degradation mechanism on Fe-Ni/CNTs for removal of 2,4-dichlorophenol in aqueous solution. Environ Sci Pollut Res 26:8768–8778. https://doi.org/10.1007/s11356-019-04394-w
Tobiszewski M, Zabrocka W, Bystrzanowska M (2019) Diethyl carbonate as a green extraction solvent for chlorophenol determination with dispersive liquid-liquid microextraction. Anal Method 11:844–850. https://doi.org/10.1039/c8ay02683a

Varsha M, Kumar PS, Rathi BS (2022) A review on recent trends in the removal of emerging contaminants from aquatic environment using low-cost adsorbents. Chemosphere 287:132270. https://doi.org/10.1016/j.chemosphere.2021.132270

Wang RX, Li MZ, Liu T, Li XY, Zhou L, Tang L, Gong CY, Gong X, Yu KF, Li N, Zhu WK, Chen T (2022a) Encapsulating carbon-coated nano zero-valent iron particles with biomass-derived carbon aerogel for efficient uranium extraction from uranium-containing wastewater. J Clean Prod 364:132654. https://doi.org/10.1016/j.jclepro.2022.132654

Wang H, Tian T, Wang D, Xu F, Ren W (2022b) Adsorption of bisphenol A and 2,4-dichlorophenol onto cetylpyridinium chloride-modified pine sawdust: a kinetic and thermodynamic study. Environ Sci Pollut Res 29:18932–18943. https://doi.org/10.1007/s11356-021-17157-3

Wang ZB, Ren DJ, Yu HY, Jiang S, Cheng YH, Zhang SQ, Zhang XQ (2021a) Adsorption kinetic and isothermal studies of 2,4-Dichlorophenol from aqueous solutions with zeolitic imidazolate framework-8 (ZIF-8). Environ Eng Sci 38:537–546. https://doi.org/10.1089/ees.2020.0286

Wang JL, Liu X, Yang MM, Han HY, Zhang SS, Ouyang GF, Han RP (2021b) Removal of tetracycline using modified wheat straw from solution in batch and column modes. J Mol Liq 338:116698. https://doi.org/10.1016/j.molliq.2021.116698

Yang YL, Cannon FS (2021) Preparation of activated carbon from pine sawdust with hydrothermal-pressure preconditioning. J Environ Chem Eng 9:106391. https://doi.org/10.1016/j.jece.2021.106391

Zhao JJ, Shen XJ, Domene X, Alcaniz JM, Liao X, Palet C (2019) Comparison of biochars derived from different types of feedstock and their potential for heavy metal removal in multiple-metal solutions. Sci Rep 9:12. https://doi.org/10.1038/s41598-019-46234-4

Zheng P, Zhang KQ, Dang Y, Bai B, Guan WS, Suo YR (2015) Adsorption of organic dyes by TiO_2@Yeast-Carbon composite microspheres and their in situ regeneration evaluation. J Nanomater 2015:13. https://doi.org/10.1155/2015/498304

Zhou LQ, Xu ZJ, Yi K, Huang QY, Chai KG, Tong ZF, Ji HB (2019) Efficient remediation of 2,4-dichlorophenol from aqueous solution using beta-cyclodextrin-based submicron polymeric particles. Chem Eng J 360:531–541. https://doi.org/10.1016/j.cej.2018.11.196